Crystalline state, Microstructure and Electrical Properties of Nickel Ferrite

Than Than Swe[*], Myint Myint Swe[**], Aye Yu New[***]

Abstract

Nickel ferrite ($NiFe_2O_4$) nanoparticles were prepared by the use of solid state reaction method. Analar(AR) grade nickel oxide (NiO) and iron III oxide (Fe_2O_3) were used to prepare the nickel ferrite ($NiFe_2O_4$) sample. The mixed powders were annealed at temperature 1000℃ for 8h. The X–ray analysis was carried out to confirm the phase formation of the sample. The average crystallite sizes were also estimated by using collected XRD lines to investigate the nanosized ferrite particles. The surface morphology of nickel ferrite ($NiFe_2O_4$) nanoparticles was characterized by Scanning Electron Microscopy (SEM). The frequency dependence of capacitance and resistance of the ferrite sample were measured by LCR meter and then used to calculate the electrical conductivity, resistivity and dielectric constant for the nickel ferrite sample.

Key words: $NiFe_2O_4$, XRD, SEM, Dielectric constant

Introduction

Ferrites with the spinel structure form a group of technologically important materials. There are many methods for the preparation of ferrites, including conventional ceramic method (solid–state reaction), co–precipitation method, hydrothermal method, high–energy ball milling method and sol–gel method. Nickel ferrites are well–known soft magnetic materials, which are based on iron oxide. They are also called ferrite magnets and could not be easily replaced by any other magnet. Cubic nickel ferrites having the chemical formula of $NiFe_2O_4$ are widely used in magnetic recording media, microwave devices and electromagnetic shielding fields. Nickel ferrite possesses relatively high Curie temperature.

[*] Associate professor, Dr, Department of Physics, Yadanabon University

[**] Lecturer, Dr, Department of Physics, Yadanabon University

[***] Lecturer, Dr, Department of Physics, Magwe University

Experimental Details

Nickel ferrite ($NiFe_2O_4$) powders have been prepared by standard solid state reaction method. For preparing the $NiFe_2O_4$ powder, pure nickel oxide (NiO) and iron (III) oxide (Fe_2O_3) were chosen as starting materials. The starting materials were weighed with digital balance and these powder materials were mixed 50g each equal ratio in mass. This mixed powder was ground by using agate motor for 5h to be homogeneous. After mixing process the powders were annealed at 1000℃ for 8h. After annealing, the powders were ground again till the fine powders were obtained. The as–prepared sample was characterized by X–ray diffraction (XRD) method to study the structural property of the sample. The as–prepared Nickel ferrite, $NiFe_2O_4$, powders were made pellet by using hydraulic press (∼70MPa). After that it was annealed at 1000℃ for 3h. For electrical measurement, silver electrode was used. Finally, dielectric measurement of the sample was measured simultaneously as a function of frequency (1 kHz – 100 kHz) using LCR meter (GW INSTEK LCR–8110G).

Results and Discussions

In the present work, powder XRD patterns of Nickel ferrite ($NiFe_2O_4$) are shown in Figure 1. The observed XRD patterns are found to agree with JCPDS and the collected XRD lines are well assigned. The appearance of the diffraction peaks demonstrates the single–phase Nickel ferrite ($NiFe_2O_4$) powders. From all XRD profiles, it was significantly obvious that the pure $NiFe_2O_4$ structure was formed at 1000℃ for 8h. The collected five peaks of the $NiFe_2O_4$ sample were (220), (311), (400), (511) and (440) respectively. The peak height was roughly proportional to the ray intensity. The intensity of (311) reflection was the strongest of all the reflections. The lattice parameters of the sample were evaluated by using crystal utility of the equation of

$$\frac{sin^2\theta}{(h^2+k^2+l^2)} = \frac{\lambda^2}{4a^2}$$

where, "θ" is the diffraction angle, (hkl) is the Miller indices, "a" is the lattice parameter and "λ" is the wavelength of incident X–ray. XRD patterns indicate the samples belong to cubic structure. The lattice parameters observed in the present investigation were a = b = c = 8.34 Å. This value was in good agreement with the reported value earlier. The crystallite sizes of the samples have been estimated by using the Scherrer's formula,

$$t = \frac{0.9\lambda}{B\ cos\theta}$$

where t is the crystallite size (nm), λ is the wavelength of incident X–ray (nm), θ is diffraction angle and B is observed FWHM (radian). The average crystallite sizes of the sample were obtained about 39.08 nm and it showed the nanosized materials.

The surface morphology and microstructural properties of $NiFe_2O_4$ powder were investigated by using Scanning Electron Microscopy (SEM). Figure 2 showed the micrographs of $NiFe_2O_4$ powder annealed at (1000℃). The surfaces were seen to be crack free and uniformly distributed in continuity. The average grain size of the $NiFe_2O_4$ was found to be about 475.87nm. It could be seen that the crystallite size of the sample was extremely fine, on the order 100 to 500nm. It was obvious that the grain distributed on the $NiFe_2O_4$ powder was observed to be dense and smooth.

To observe the dielectric properties of $NiFe_2O_4$ samples, capacitance and dissipation factor were measured by using LCR meter at applied frequency ranging from 1 kHz to 100 kHz under zero bias condition.

Table (1) The values of capacitance and dissipation factor for $NiFe_2O_4$ sample

Frequency (kHz)	Capacitance (pF)	Dissipation factor
1	41.62	20.19
25	12.28	3.01
50	11.27	1.67
75	11.04	1.18
100	10.86	0.95

From above data, the values of capacitance depend on applied frequencies. Figures (3–4) showed the variations of capacitance versus frequency of $NiFe_2O_4$ sample and dissipation factor verses frequency of $NiFe_2O_4$ sample From these figure, it was obvious that the capacitance and dissipation factor decreased with increase in frequencies. We determined that the dielectric constant εr by using the following equation,

$$\varepsilon_r = \frac{Cd}{\varepsilon_0 A}$$

where, C is capacitance, d is the thickness of sample, A is the surface area and ε_0 is the permittivity of free space. Then, we determined that the loss dielectric or loss tangent by using the following equation, $\tan\delta = \frac{D}{\varepsilon_r}$ where, $\tan\delta$ = dielectric loss , D = dissipation factor, ε_r = dielectric constant.

Table (2) The values of dielectric constant and dielectric loss for $NiFe_2O_4$ sample

Frequency (kHz)	Dielectric constant	Dielectric loss
1	108.09	0.19
25	31.87	0.09
50	29.28	0.06
75	28.68	0.04
100	28.22	0.03

From these data, the values of dielectric constant and dielectric loss depend on applied frequency. Dielectric constant and dielectric loss versus frequency of $NiFe_2O_4$ samples as shown in Figures 5 (a−b). From these figures, the dielectric constant and dielectric loss decreased with increasing applied frequencies.

To investigate the resistivity and electrical conductivity of $NiFe_2O_4$ samples were calculated by using the following equation, $\rho = \frac{1}{\sigma} = \frac{RA}{l}$

where, l is the thickness of the sample, A is the cross–sectional area of the electrodes and R is the resistance.

Table (3) The values of resistivity and conductivity for $NiFe_2O_4$ sample

Frequency (kHz)	Resistivity (kΩm)	Conductivity (μS/m)
1	8.20	121.93
25	7.60	131.54
50	7.30	136.95
75	7.07	141.40
100	6.79	147.26

Resistivity and conductivity versus frequency of $NiFe_2O_4$ sample as shown in Figure 6. From these figures, the resistivity of the samples decreased with increase conductivity.

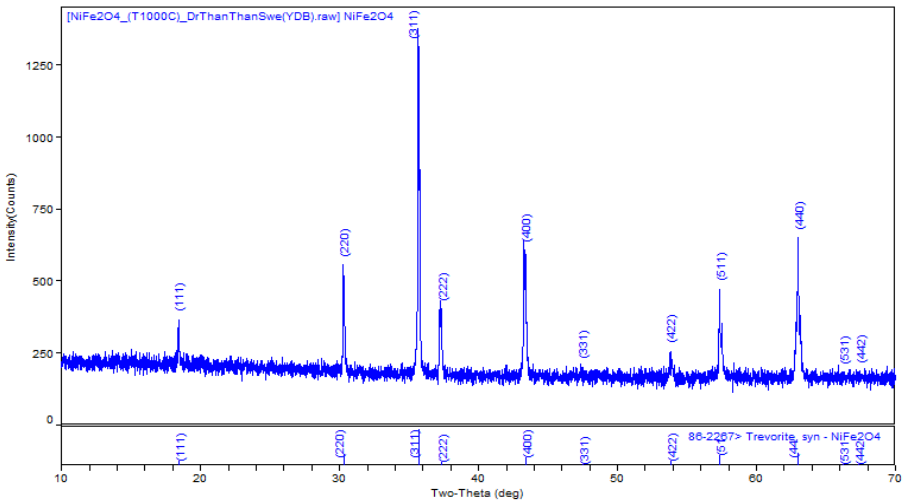

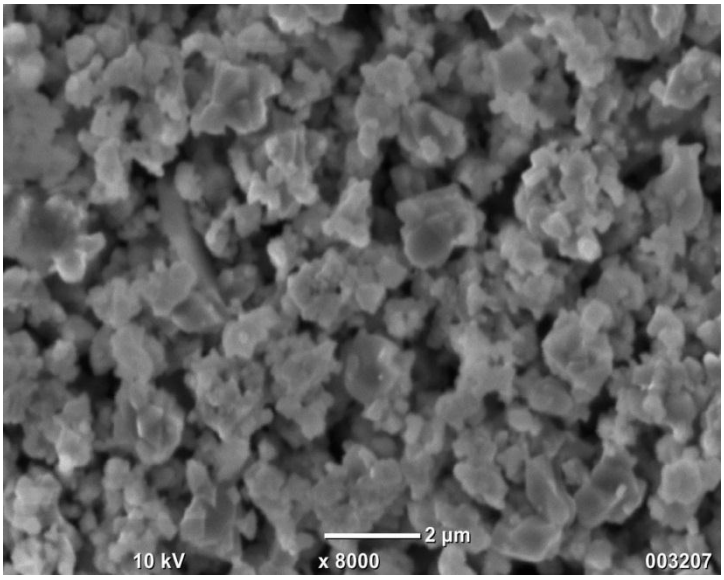

Figure (2) Scanning Electron Microscope image of

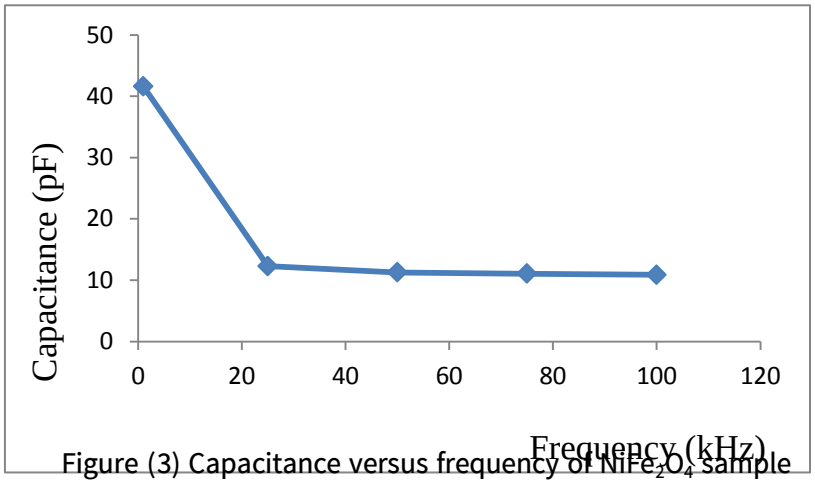

Figure (3) Capacitance versus frequency of $NiFe_2O_4$ sample

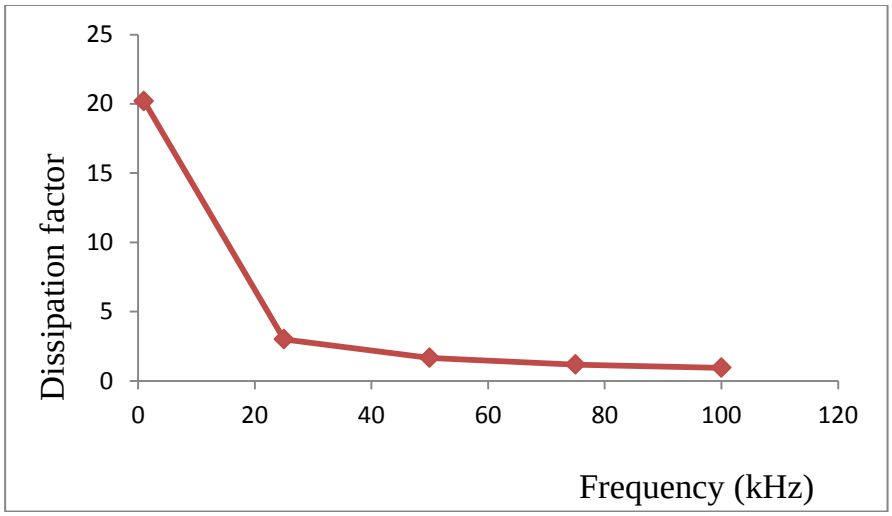

Figure (4) Dissipation factor versus frequency of $NiFe_2O_4$ sample

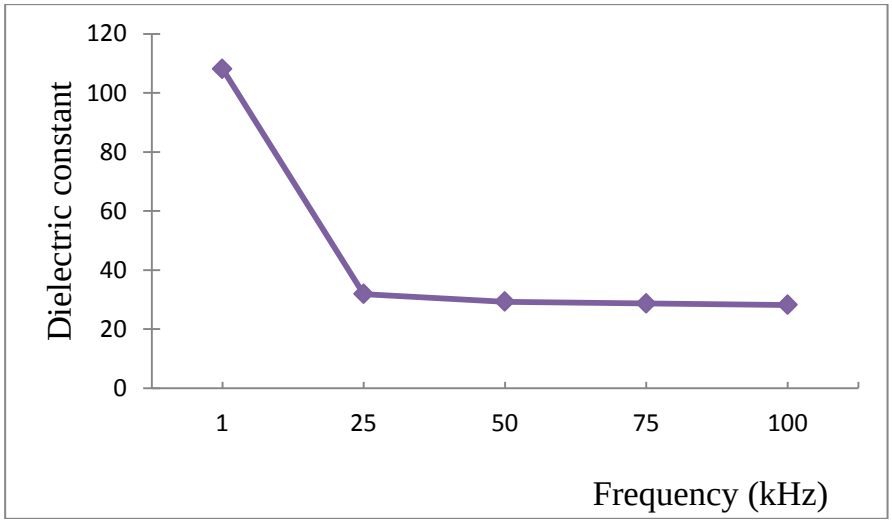

Figure (5a) Dielectric constant versus frequency of $NiFe_2O_4$ sample

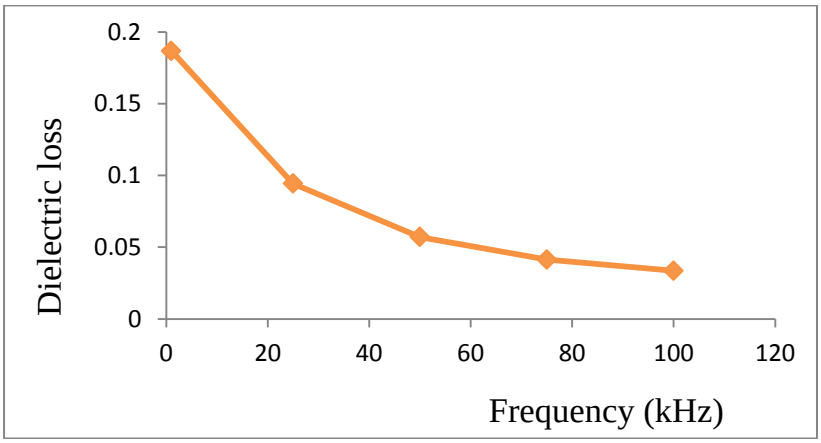

Figure (5b) Dielectric losses as a function of frequency of $NiFe_2O_4$

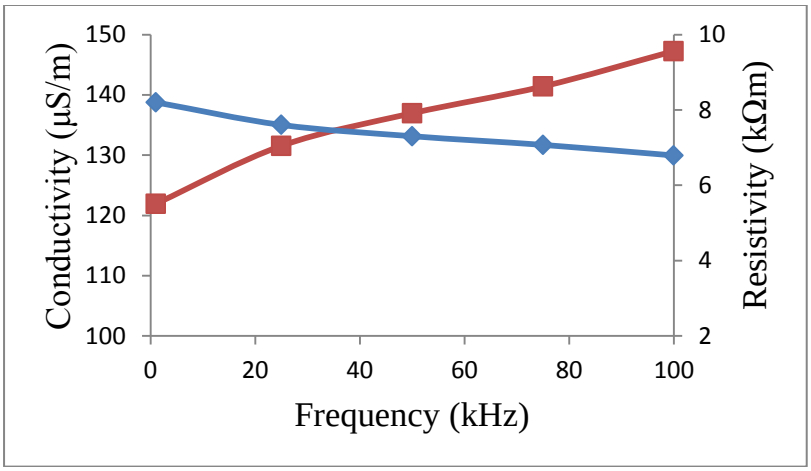

Figure (6) Resistivity and conductivity versus frequency of $NiFe_2O_4$

Conclusion

Growth and characterization of nickel ferrite powders were successfully investigated. The results obtained from the X–ray diffraction pattern, nickel ferrite powders were polycrystalline with a cubic structure and the lattice parameter 'a' was 8.34 Å. The crystallite sizes were found to be the nanosized materials because the obtained crystallite sizes were in the range from 23.75 nm to 45.99 nm. From the scanning electron microscopy measurement, the surfaces were seen to be crack free and uniformly distribute in continuity. The average grain sizes of nickel ferrite were found to be about 475.87nm. It was obvious that the grain distributed on the nickel ferrite powder was dense and smooth. The dielectric properties of $NiFe_2O_4$ samples were studied in terms of dissipation factor and dielectric constant. From capacitance frequency measurements, the values of capacitance depended on applied frequencies. From dissipation factor versus frequency of $NiFe_2O_4$ samples, it was obvious that the dissipation factor decreased with the increase in frequencies. The results are ε_r–f and tanδ–f characteristics curves and it was observed that dielectric constant and loss tangent decreased with increasing applied frequencies. From the graphs of ρ–f and σ–f, the sample exhibit decrease in resistivity with the increase in frequency, whereas conductivity increased with increase in applied frequencies. The results show that $NiFe_2O_4$ sample was suitable among several ferrite materials for high frequency applications.

Acknowledgements

We would like to thank Dr Si Si Khin, acting–Rector & Dr Tint Moe Thuzar, Pro–Rector of Yadanabon University for their encouragement. We are grateful to the full support of Dr Yi Yi Myint, Professor, Head of Physics Department, and Dr May Thidar Win, Professor, Department of Physics, Yadanabon University.

References

Cornell, R. M., Schwertmann, U. The Iron Oxides. WILEY–VCH verlag Gm–bH & Co. KGaA Weinheim, 2003

Cullity, B. D. (1978) "Elements of X–Ray Diffraction", Wesley Reading

F. Haaberey, J. Appl. Phys., 40 (1969) 2835

Faleevm S. V; van Schilfgaarde, M; Kotani, T. Phys Rev Lett 2004, 93, 126406

G. A. Niklasson and Clase G. Granqvist, J. Mater. Chem. 17 (2007) 127

G. Moltgen, Z. Angew, Phys. , 4 (1952) 216

Hostetter J. C. and Roberts H. S. J Ame. Cera. Soc. 4 927